Engineering Fracture Mechanics Vol. 23, No. 6, pp. 1051–1065, 1986
Printed in Great Britain.

0013–7944/86 $3.00 + .00

STRESS CONCENTRATION OF A STRIP WITH DOUBLE EDGE NOTCHES UNDER TENSION OR IN-PLANE BENDING

HIRONOBU NISITANI
Faculty of Engineering, Kyushu University, Fukuoka 812, Japan

and

NAO-AKI NODA
Department of Mechanical Engineering, Kyushu Institute of Technology, Kitakyushu 804, Japan

Abstract—The stress concentration analysis of 60° V-shaped or partially-circular double edge notches in an infinite strip under tension or in-plane bending is discussed. The stress field induced by a point force in an infinite plate is used to solve these problems. The present results for semicircular notch are in close agreement with other reports. The results calculated on the 60° V-shaped notches show that the Neuber formula gives an underestimated stress concentration factor of about 11% for tension case and in about 9% for bending case. These errors exist for a wide range of notch depth. However, in the case of blunt notches, the Neuber solution of deep hyperbolic notches still gives a sufficient accuracy in engineering use. In addition, the stress concentration factors of 60° V-shaped notches are also represented by diagrams for wide use.

NOTATION

ρ	root radius of notch
t	depth of notch
ω	flank angle of notch
W	width of strip
w	minimum width of strip
(x, y)	coordinates of a point in question
(ξ, η)	coordinates of a point where a point force acts
P, Q	magnitude of a point force
p, q	magnitude of surface force
ρ_x, ρ_y	density of body force
σ^P, σ^Q	stresses due to a point force
σ^p, σ^q	stresses due to surface force
n_t	total division number
σ_n	nominal stress for the minimum width w
K_t	stress concentration factor (SCF) based on the minimum width w
K_{tN}	SCF of the Neuber formula
K_{tE}	SCF of an elliptic hole in an infinite plate
K_{tH}	SCF of deep hyperbolic notches in an infinite plate
K_{tV}	SCF of a 60° V-shaped notch in a semi-infinite plate
K_{tSE}	SCF of a semi-elliptical notch in a semi-infinite plate

1. INTRODUCTION

A DOUBLE EDGE notched strip shown in Fig. 1 is widely used as a fatigue test specimen of metals. Ling[1–3], Tamate[4], Isida[5, 6] and Atsumi[7] have carried out the stress analyses of semicircular notches in a strip. Frocht[8] and Kikukawa[9] have investigated U-shaped notches by experiment. Moreover, Nisitani[10] and Hasebe[11] have analyzed semi-elliptical notches. In this way, many researchers have tried to obtain the stress concentration factors K_t of this problem over a long period. However, most of the research on this problem has treated only a few notch sizes by experiment or calculation; namely, there are few papers in which the accurate stress concentration factors are shown under various geometrical conditions necessary for design or research. Therefore, the so-called Neuber's trigonometric formula eqn (1), which gives approximate values of K_t[12], has been used for more than 40 years:

$$K_{tN} = \frac{(K_{tE}-1)(K_{tH}-1)}{\sqrt{((K_{tE}-1)^2+(K_{tH}-1)^2)}}+1, \tag{1}$$

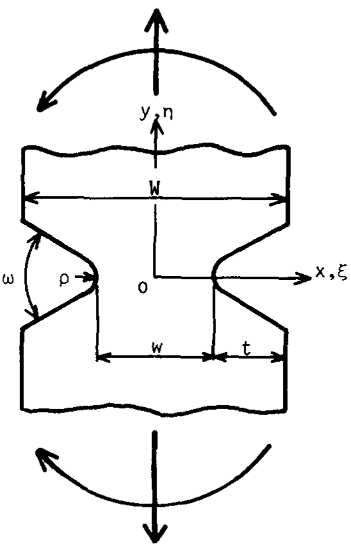

Fig. 1. A double edge notched strip under tension or in-plane bending.

where K_{tE} and K_{tH} are expressed as follows.

(1) In tension problem:

$$K_{tE} = 1+2\sqrt{\left(\frac{t}{\rho}\right)}$$

$$K_{tH} = \frac{2\left(\frac{w}{2\rho}+1\right)\sqrt{\left(\frac{w}{2\rho}\right)}}{\left(\frac{w}{2\rho}+1\right)\tan^{-1}\sqrt{\left(\frac{w}{2\rho}\right)}+\sqrt{\left(\frac{w}{2\rho}\right)}}. \tag{2}$$

(2) In bending problem:

$$K_{tE} = 1+2\sqrt{\left(\frac{t}{\rho}\right)}$$

$$K_{tH} = \frac{4\frac{w}{2\rho}\sqrt{\left(\frac{w}{2\rho}\right)}}{3\left\{\sqrt{\left(\frac{w}{2\rho}\right)}+\left(\frac{w}{2\rho}-1\right)\tan^{-1}\sqrt{\left(\frac{w}{2\rho}\right)}\right\}}. \tag{3}$$

In this paper, the stress concentration problems of 60° V-shaped and partially-circular double edge notches in an infinitely long strip under tension or in-plane bending are analyzed by the body force method[13–15]. Recently, Nisitani[10] and Hasegawa[16] showed the method of analysis for semicircular and partially-elliptic-arc notches in a strip. In their analysis the boundary conditions at the straight edges of a strip are completely satisfied because they used Green's function of an infinite strip. However, since the Green's function of a strip cannot be given in closed form, their analysis is not convenient for calculating systematically the stress concentration factors under various geometrical conditions. Taking account of this point, we apply the stress field of a point force in a semi-infinite plate (Green's function) to the strip problems in this paper. Since the Green's function of a semi-infinite plate can be obtained in closed form, the accurate stress concentration factors necessary for design or research can be calculated with short CPU time. As a result, systematically calculated K_t values of 60° V-shaped notches can be represented by tables and diagrams for wide use.

2. METHOD OF ANALYSIS

The body force method can generally analyze all kinds of two dimensional problems by using the stress field of a point force in an infinite plate as a fundamental solution[13, 14]. The given boundary conditions are satisfied by distributing the body force (continuously embedded point forces) along the imaginary boundaries in an infinite plate and adjusting its density so as to satisfy the specified conditions. The imaginary boundary stands for the prospective boundary for hole or notch which should be free from stresses.

In solving a strip problem, Nisitani[10] and Hasegawa[16] used the stress field of a point force in an infinitely long strip (i.e. Green's function of a strip) as a fundamental solution. If we use this solution in the present analysis, the boundary conditions have only to be satisfied at the prospective boundary for double edge notches imagined in an unnotched strip. However, the Green's function of a strip cannot be given in closed form; thus the function must be evaluated numerically in the analysis. Accordingly, in the present paper, we use the stress field of a point force in a semi-infinite plate as a fundamental solution.

Figure 2 shows the method of analysis proposed in this paper. Consider two kinds of semi-infinite plates: one is defined in the range $-W/2 \leqslant x < \infty$ (Fig. 2(b)), and the other is defined in the range $-\infty < x \leqslant W/2$ (Fig. 2(c)). The edges $x = \pm W/2$ correspond to the stress free edges of the strip shown in Fig. 2(a). The stress fields of a point force in the semi-infinite plates shown in Figs. 2(b), (c) can be given in closed form[13].

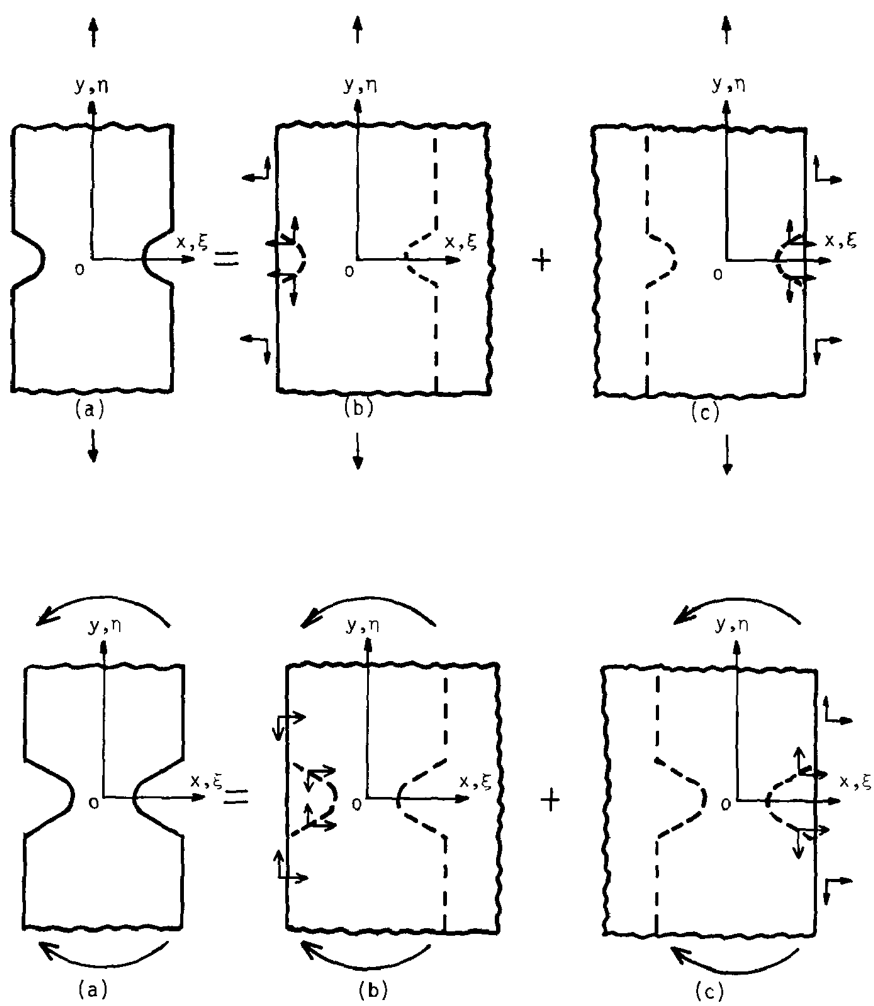

Fig. 2. Illustration of the present method of analysis. (a) A double edge notched strip; (b), (c) semi-infinite plates distributed body forces and surface forces.

The boundary conditions for notch and edge of the strip in the range of $x < 0$ are satisfied by using the Green's function of a semi-infinite plate shown in Fig. 2(b). On the other hand, the boundary conditions in the range of $x > 0$ are satisfied by using the Green's function of a semi-infinite plate shown in Fig. 2(c). As a result, the method of analysis in this paper is reduced to determining the densities of body force (for notch) and of surface force (for strip edge) distributed in the semi-infinite plates shown in Fig. 2(b) and Fig. 2(c).

In the present analysis, the density of surface force distributed at the prospective boundary for the strip edge is small, especially for shallow notches. This means the accuracy of the present analysis is improved by using the Green's function of a semi-infinite plate as a fundamental solution. Moreover, the CPU time necessary for calculating the accurate stress concentration factors is short because the fundamental solutions is given in closed form.

3. FUNDAMENTAL SOLUTIONS AND DEFINITION OF BODY FORCE DENSITY

When a point force P, Q acts at a point (ξ, η) in a semi-infinite plate shown in Fig. 3(a) or Fig. 3(b), the stresses at (x, y) are given by eqn (4):

$$\sigma_x^P = \frac{\bar{P}}{2\pi}\left[\tfrac{1}{2}[-(\bar{x}-\bar{\xi})\{(\bar{y}-\bar{\eta})^2+3(\bar{x}-\bar{\xi})^2\}r_1^{-4}+(\bar{x}+\bar{\xi})\{(\bar{y}-\bar{\eta})^2+3(\bar{x}+\bar{\xi})^2\}r_2^{-4}]\right.$$
$$\left.-\frac{1}{\bar{x}(A^2+n^2)^3}\{(n-1)A^4+2n(2n^2-3n+3)A^2+n^3(3n^2+3n-2)\}\right],$$
$$\sigma_y^P = \frac{\bar{P}}{2\pi}\left[\tfrac{1}{2}[(\bar{x}-\bar{\xi})\{(\bar{x}-\bar{\xi})^2-(\bar{y}-\bar{\eta})^2\}r_1^{-4}-(\bar{x}+\bar{\xi})\{(\bar{x}+\bar{\xi})^2-(\bar{y}-\bar{\eta})^2\}r_2^{-4}]\right.$$
$$\left.-\frac{1}{\bar{x}(A^2+n^2)^3}\{(n+3)A^4+2n(2n^2+3n-3)A^2+n^3(3n^2-5n+2)\}\right],$$
$$\tau_{xy}^P = \frac{\bar{P}}{2\pi}\left[\tfrac{1}{2}(\bar{y}-\bar{\eta})[\{(\bar{y}-\bar{\eta})^2+3(\bar{x}-\bar{\xi})^2\}r_1^{-4}+\{(\bar{y}-\eta)^2+3(\bar{x}+\bar{\xi})^2\}r_2^{-4}]\right.$$
$$\left.+\frac{2A}{\bar{x}(A^2+n^2)^3}\{(n+1)A^2+n^2(5n-3)\}\right], \tag{4a}$$
$$\sigma_x^Q = \frac{\bar{Q}}{2\pi}\left[\tfrac{1}{2}(\bar{y}-\bar{\eta})[\{(\bar{y}-\bar{\eta})^2-(\bar{x}-\bar{\xi})^2\}r_1^{-4}+\{(\bar{y}-\bar{\eta})^2-(\bar{x}+\bar{\xi})^2\}r_2^{-4}]\right.$$
$$\left.+\frac{A}{\bar{x}(A^2+n^2)^3}\{A^4+2(3n-1)A^2-n^2(n^2+2n-6)\}\right],$$
$$\sigma_y^Q = \frac{\bar{Q}}{2\pi}\left[-\tfrac{1}{2}(\bar{y}-\bar{\eta})[\{3(\bar{y}-\bar{\eta})^2+(\bar{x}-\bar{\xi})^2\}r_1^{-4}+\{3(\bar{y}-\bar{\eta})^2+(\bar{x}+\bar{\xi})^2\}r_2^{-4}]\right.$$
$$\left.+\frac{A}{\bar{x}(A^2+n^2)^3}\{A^4-2(n-1)A^2-n^2(n^2-6n+6)\}\right],$$
$$\tau_{xy}^Q = \frac{\bar{Q}}{2\pi}\left[-\tfrac{1}{2}[(\bar{x}-\bar{\xi})\{3(\bar{y}-\bar{\eta})^2+(\bar{x}-\bar{\xi})^2\}r_1^{-4}+(\bar{x}+\bar{\xi})\{3(\bar{y}-\bar{\eta})^2+(\bar{x}+\bar{\xi})^2\}r_2^{-4}]\right.$$
$$\left.+\frac{1}{\bar{x}(A^2+n^2)^3}\{-A^4+6n(n-1)A^2-n^3(n-2)\}\right], \tag{4b}$$

where

$$r_1^2 = (\bar{x}-\bar{\xi})^2+(\bar{y}-\bar{\eta})^2, \qquad r_2^2 = (\bar{x}+\bar{\xi})^2+(\bar{y}-\bar{\eta})^2,$$
$$A = (\bar{y}-\bar{\eta})/\bar{x}, \qquad n = 1+\bar{\xi}/\bar{x},$$
$$\bar{x} = x+W/2,\quad \bar{y} = -y,\quad \bar{\xi} = \xi+W/2,\quad \bar{\eta} = -\eta\quad \bar{P} = P,\quad \bar{Q} = -Q \qquad \text{[case in Fig. 3(a)]},$$
$$\bar{x} = -x+W/2,\quad \bar{y} = y,\quad \bar{\xi} = -\xi+W/2,\quad \bar{\eta} = \eta\quad \bar{P} = -P,\quad \bar{Q} = Q \qquad \text{[case in Fig. 3(b)]}.$$

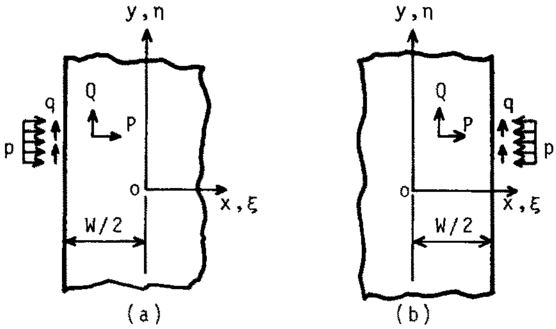

Fig. 3. Point forces acting in a semi-infinite plate and surface forces distributing on a semi-infinite plate.

On the other hand, when surface forces p, q are distributed at the surface ($\eta = \eta_1 \sim \eta_2$) of the semi-infinite plate shown in Fig. 3(a) or Fig. 3(b), the stresses at (x, y) are given as follows:

$$\sigma_x^p = \frac{p}{\pi}\{\tfrac{1}{2}(\sin 2\phi_2 - \sin 2\phi_1) + \phi_2 - \phi_1\},$$

$$\sigma_y^p = \frac{p}{\pi}\{\phi_2 - \phi_1 + \tfrac{1}{2}(\sin 2\phi_1 - \sin 2\phi_2)\}, \tag{5a}$$

$$\tau_{xy}^p = \frac{p}{2\pi}\{\cos 2\phi_1 - \cos 2\phi_2\},$$

$$\sigma_x^q = \frac{q}{2\pi}\{\cos 2\phi_1 - \cos 2\phi_2\},$$

$$\sigma_y^q = -\frac{2q}{\pi}\left\{\tfrac{1}{4}(\cos 2\phi_1 - \cos 2\phi_2) + \ln\frac{|\cos\phi_2|}{|\cos\phi_1|}\right\}, \tag{5b}$$

$$\tau_{xy}^q = \frac{q}{\pi}\{\phi_2 - \phi_1 + \tfrac{1}{2}(\sin 2\phi_1 - \sin 2\phi_2)\},$$

where

$$\phi_1 = \tan^{-1}\frac{\eta_1 - y}{\xi - x}, \qquad \phi_2 = \tan^{-1}\frac{\eta_2 - y}{\xi - x}.$$

By using the fundamental solutions shown in eqns (4) and (5) the present method of analysis is reduced to determining the densities of body force distributed along the prospective boundary for notch and strip edge. The densities ρ_x, ρ_y of the body force distributed in the x-, y-directions are defined as follows.

(1) Definition of the body force density (for notch):

$$\rho_x = \frac{dF_\xi}{d\eta}, \qquad \rho_y = -\frac{dF_\eta}{d\xi} \qquad \text{(tension)},$$
$$\rho_x = \frac{dF_\xi}{d\eta}, \qquad \rho_y = \frac{w}{2\xi}\frac{dF_\eta}{d\xi} \qquad \text{(in-plane bending)}. \tag{6}$$

(2) Definition of the surface force density (for strip edge):

$$\rho_x = \frac{dF_\xi}{ds}, \qquad \rho_y = \frac{dF_\eta}{ds}. \tag{7}$$

In eqns (6) and (7), dF_ξ, dF_η denote the x-, y-components, respectively, of the body force distributing along the infinitesimal element $ds\ \{=\sqrt{((d\xi)^2 + (d\eta)^2)}\}$.

The densities ρy of the bending problem are defined considering the bending stress field:

$$\sigma_y^\infty = \frac{2x}{\xi}\sigma_0, \tag{8}$$

where σ_0 is a constant corresponding to the magnitude of the bending stress. In the present analysis, the stepped distribution (constant in each interval) of the body force is substituted for the continuously varying distribution. In this procedure, the definition of the body force densities, which make the stepped distribution approximately constant at each interval, should be used. From this viewpoint, the definition of eqns (6) and (7) are used in the present analysis.

Recently, many researchers have frequently used numerical methods making use of the fundamental solutions similar to those of the body force method; e.g. boundary element method (BEM). However, in the body force method, the unique idea of the body force density enables us to obtain very accurate solutions.

4. RESULTS AND DISCUSSION

Computer program for the analysis of double V-shaped notches in a strip was coded using the fundamental solutions given in Section 3. It is difficult to determine in closed form the body force densities satisfying the boundary conditions completely; therefore, the imaginary boundaries are divided and the problem is solved numerically. The densities of the body force, which are assumed to be constant in each interval, are determined from the boundary condition at the midpoint of each interval. Since the error due to the finiteness of the division number n_t is nearly proportional to $1/n_t$[13, 14], the value of the stress concentration factor corresponding to $n_t \to \infty$ is obtained by extrapolation of the two values of K_t corresponding to the two finite values of n_t.

In the following discussion, we use the stress concentration factors (SCFs) based on the net section of width w. They are expressed as follows.

(1) In the tension problem:

$$K_t = \frac{\sigma_{max}}{\sigma_n}, \qquad \sigma_n = \frac{P}{w}, \tag{9}$$

where P is the magnitude of external load.

(2) In the in-plane bending problem:

$$K_t = \frac{\sigma_{max}}{\sigma_n}, \qquad \sigma_n = \frac{6M}{w^2}, \tag{10}$$

where M is the magnitude of external bending moment. Here σ_{max} is the maximum stress at the root of notches and σ_n is the nominal stress for the minimum width w.

4.1 *SCF of semicircular notch*

There are many reports concerning the problems of semicircular notch. Therefore, by comparing them with the present results, the accuracy of the present analysis can be estimated. In Tables 1 and 2, SCFs of semicircular notches in strips under tension and in-plane bending are shown. The results of Hasegawa [16], Ling [1–3] and Isida [5, 6] are in close agreement with the present results. The results in Tables 1 and 2 are plotted in Figs. 4 and 5, respectively. In Figs. 4 and 5, Neuber's corresponding values (eqn (1), $K_{tE} = 3.065$) are designated by the dashed line.

4.2 *SCF of partially-circular notch*

In Tables 3 and 4, SCFs of partially-circular notches in a strip with a minimum width $w = 10$ mm are shown. These specimens are frequently used for fatigue tests of metals. The values due to the Neuber formula K_{tN} and the values of deep hyperbolic notches K_{tH} are also shown to be compared with the values of the present analysis. It is found that the solution of deep hyperbolic notch [eqn (2)] gives a sufficient accuracy for blunt notches.

Table 1. SCFs of semicircular notches under tension.

2ρ/W	Present analysis	Hasegawa Tokoyoda	Nisitani	Ling	Isida	Neuber
0.02	3.003	–	–	–	3.003	3.00
0.03	2.972	–	–	–	2.971	2.96
0.05	2.907	2.908	–	–	2.907	2.88
0.1	2.745	2.7446	2.746	2.745	2.745	2.68
0.2	2.429	2.4283	2.429	2.429	2.429	2.29
0.3	2.134	2.1330	–	2.134	2.134	1.98
0.4	1.865	1.8645	1.864	1.865	1.865	1.73
0.5	1.624	1.6241	–	1.624	–	1.54
0.6	1.420	1.4192	1.420	1.420	–	1.38
0.7	1.261	1.2602	–	1.261	–	1.26
0.8	1.151	1.1501	1.151	–	–	1.16
0.9	1.070	1.0693	–	–	–	1.07

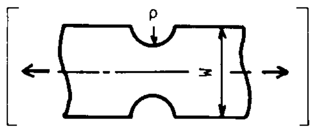

Table 2. SCFs of semicircular notches under in-plane bending.

2ρ/W	Present analysis	Ling	Isida	Neuber
0.02	2.906	–	2.91	2.91
0.03	2.833	–	2.83	2.83
0.05	2.697	–	2.70	2.68
0.1	2.408	2.409	2.41	2.34
0.2	1.985	1.986	1.98	1.90
0.3	1.693	1.694	–	1.64
0.4	1.488	1.489	–	1.46
0.5	1.341	1.344	–	1.33
0.6	1.235	1.238	–	1.23
0.7	1.155	1.158	–	1.16
0.8	1.093	–	–	1.09
0.9	1.043	–	–	1.04

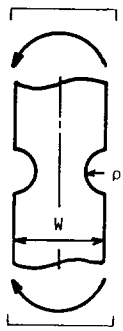

4.3 *SCF of* 60° *V-shaped notch*

Tables 5 and 6 show SCFs of 60° V-shaped notches (K_t) under tension and in-plane bending. In the case of shallow notch ($t \leqslant \rho/2$), K_t means SCF of partially-circular notch. The Neuber values K_{tN} [eqn (1)] are also shown to be compared with the K_t values. The results in Tables 5 and 6 are also shown to be compared with the K_t values. The results in Tables 5 and 6 are plotted in Figs. 6–9 so as to be useful further in design or research.

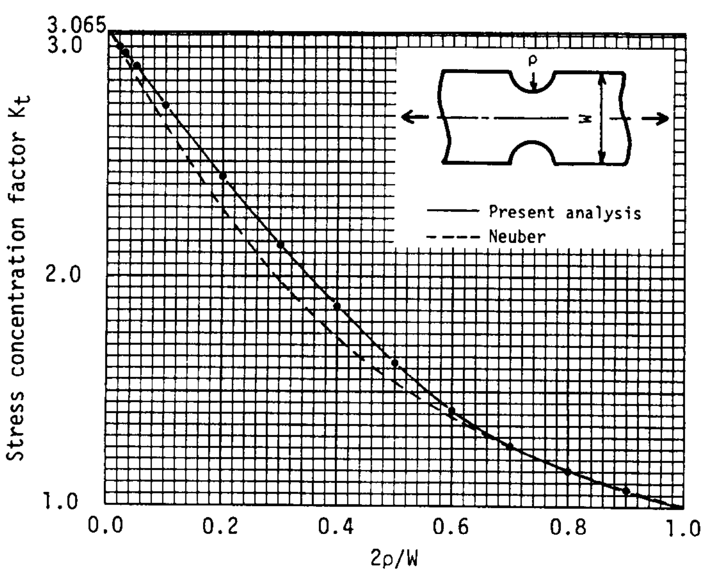

Fig. 4. SCF of semicircular notches under tension.

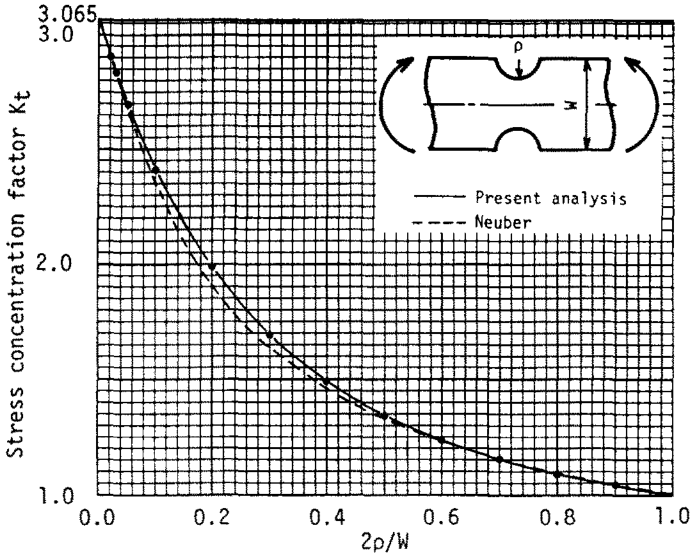

Fig. 5. SCF of semicircular notches under in-plane bending.

In Figs. 6 and 8, the ordinate represents the values of SCFs, and the abscissa represents the relative notch depth $2t/W$. Comparing the values of 60° V-shaped notch with the corresponding Neuber value, we conclude that Neuber's rule eqn (1) underestimates SCFs of the 60° V-shaped notch in about 11% for tension case and in about 9% for bending case. These errors exist for a wide range of notch depth.

The charts of SCF are also shown in different ways from Figs. 6 and 8. In Figs. 7 and 9, the abscissa represents the relative notch radius $2\rho/W$. Using these charts (Figs. 6–9), SCF K_t not calculated in this paper will be estimated.

4.4 *Relation between notch shape and stress concentration factor*

Tables 7 and 8 show the values K_t/K_{to}, where K_t means the SCF of double V-notches in a strip and K_{to} means the SCF of the notch in a semi-infinite plate (see Appendix). In Tables 7 and 8, it is

Table 3. SCFs of partially-circular notches under tension.

W(mm)	11		12		15		20		∞
ρ(mm)	K_t	K_{tN}	K_t	K_{tN}	K_t	K_{tN}	K_t	K_{tN}	K_{tH}
10	1.282	1.25	1.325	1.27	1.341	1.29	1.327	1.29	1.301
20	1.168	1.14	1.179	1.15	1.171	1.15	1.161	1.16	1.158
50	1.074	1.06	1.071	1.06	1.065	1.06	1.064	1.06	1.065
100	1.036	1.03	1.034	1.03	1.033	1.03	1.033	1.03	1.033

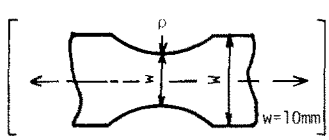

Table 4. SCFs of partially-circular notches under in-plane bending.

W(mm)	11		12		15		20		∞
ρ(mm)	K_t	K_{tN}	K_t	K_{tN}	K_t	K_{tN}	K_t	K_{tN}	K_{tH}
10	1.178	1.17	1.184	1.17	1.181	1.18	1.178	1.18	1.180
20	1.096	1.09	1.095	1.09	1.092	1.09	1.090	1.09	1.095
50	1.039	1.04	1.038	1.04	1.037	1.04	1.037	1.04	1.039
100	1.019	1.02	1.019	1.02	1.018	1.02	1.018	1.02	1.020

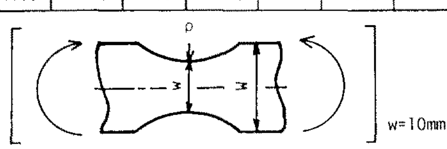

Table 5. SCFs of 60° V-shaped notches under tension.

	2ρ/W=0.02		2ρ/W=0.03		2ρ/W=0.05		2ρ/W=0.1		2ρ/W=0.2		2ρ/W=0.5		2ρ/W=1.0	
2t/W	K_t	K_{tN}	K_t	K_{tN}	K_t	K_{tN}	K_t	K_{tN}	K_t	K_{tN}	K_t	K_{tN}	K_t	K_{tN}
0.02	3.003	2.94	2.607	2.58	2.216	2.22	1.834	1.86	1.573	1.60	1.347	1.37	1.236	1.25
0.05	4.145	3.93	3.524	3.38	2.907	2.83	2.298	2.28	1.880	1.88	1.521	1.53	1.346	1.34
0.1	5.264	4.85	4.418	4.12	3.577	3.38	2.745	2.64	2.169	2.11	1.675	1.64	1.434	1.40
0.2	6.356	5.71	5.291	4.79	4.227	3.87	3.166	2.94	2.429	2.27	1.791	1.69	1.483	1.41
0.3	6.726	6.00	5.580	5.00	4.431	4.00	3.285	2.99	2.483	2.28	1.791	1.67	1.458	1.38
0.4	6.697	5.98	5.544	4.96	4.390	3.95	3.234	2.92	2.424	2.21	1.727	1.61	1.400	1.34
0.5	6.401	5.74	5.292	4.75	4.181	3.77	3.068	2.78	2.288	2.10	1.624	1.54	1.327	1.29
0.6	5.897	5.33	4.872	4.41	3.843	3.48	2.813	2.57	2.096	1.95	1.499	1.45	1.251	1.24
0.7	5.204	4.76	4.297	3.93	3.389	3.11	2.480	2.30	1.857	1.76	1.366	1.35	1.183	1.19
0.8	4.304	3.99	3.553	3.30	2.808	2.62	2.069	1.97	1.581	1.55	1.237	1.24	1.122	1.13
0.9	3.094	2.92	2.568	2.44	2.051	1.98	1.567	1.55	1.289	1.30	1.122	1.13	1.063	1.07

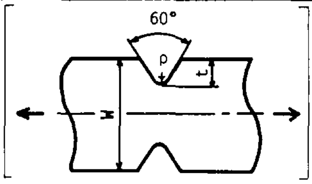

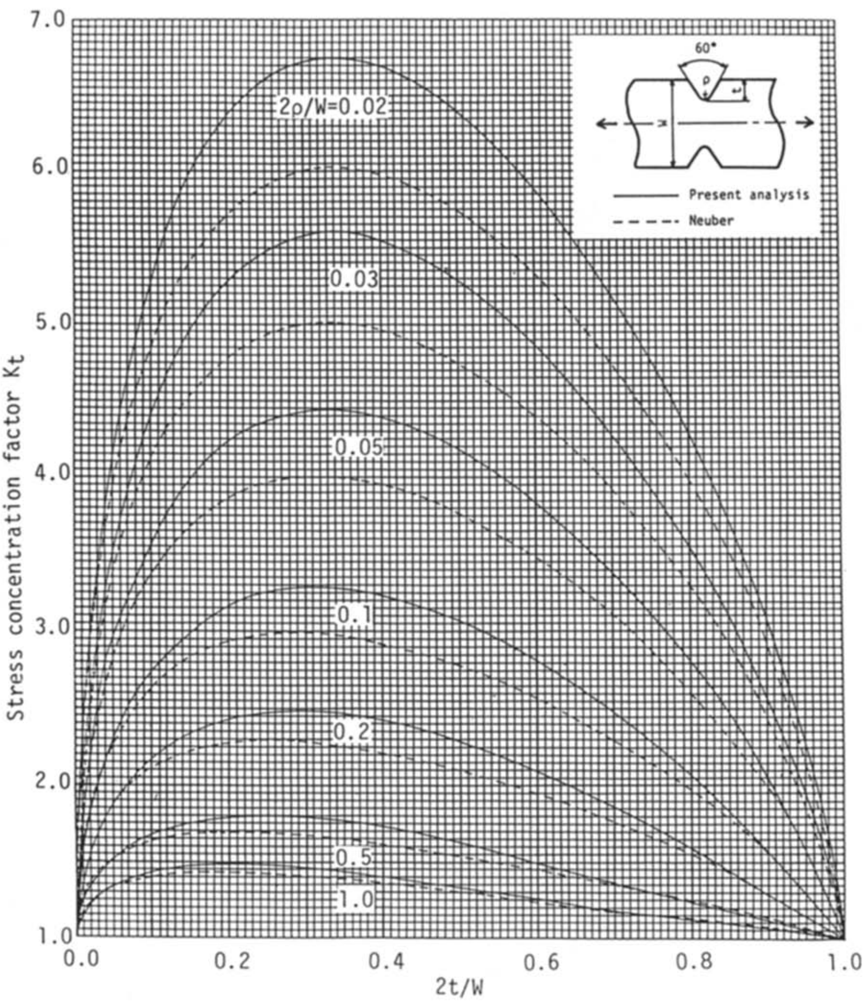

Fig. 6. SCF of 60° V-shaped notches under tension.

Table 6. SCFs of 60° V-shaped notches under in-plane bending.

	2ρ/W=0.02		2ρ/W=0.03		2ρ/W=0.05		2ρ/W=0.1		2ρ/W=0.2		2ρ/W=0.5		2ρ/W=1.0	
2t/W	K_t	K_{tN}	K_t	K_{tN}	K_t	K_{tN}	K_t	K_{tN}	K_t	K_{tN}	K_t	K_{tN}	K_t	K_{tN}
0.02	2.905	2.86	2.522	2.51	2.143	2.16	1.772	1.81	1.520	1.56	1.303	1.33	1.198	1.21
0.05	3.850	3.67	3.269	3.15	2.696	2.64	2.130	2.12	1.744	1.75	1.417	1.42	1.260	1.26
0.1	4.613	4.27	3.870	3.63	3.135	2.98	2.407	2.33	1.908	1.87	1.487	1.46	1.290	1.27
0.2	5.127	4.66	4.269	3.91	3.413	3.16	2.565	2.42	1.984	1.90	1.499	1.46	1.281	1.26
0.3	5.123	4.66	4.253	3.89	3.386	3.13	2.527	2.37	1.940	1.85	1.459	1.43	1.249	1.24
0.4	4.895	4.49	4.060	3.74	3.228	3.00	2.407	2.27	1.850	1.78	1.402	1.38	1.213	1.21
0.5	4.546	4.21	3.771	3.51	3.002	2.82	2.245	2.14	1.739	1.69	1.340	1.33	1.178	1.18
0.6	4.114	3.85	3.418	3.22	2.730	2.59	2.058	1.98	1.616	1.58	1.277	1.27	1.143	1.15
0.7	3.607	3.42	3.008	2.86	2.418	2.32	1.849	1.80	1.483	1.47	1.213	1.21	1.109	1.11
0.8	3.007	2.88	2.526	2.43	2.056	2.00	1.614	1.59	1.340	1.33	1.146	1.15	1.073	1.08
0.9	2.244	2.18	1.920	1.87	1.614	1.59	1.340	1.33	1.182	1.18	1.075	1.08	1.037	1.04

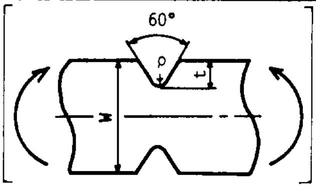

Table 7. Values $K_t/K_t|_{2t/W\to 0}$ in tension of a strip.

2ρ/W \ 2t/W	0.02	0.03	0.05	0.1	0.2	0.5	1.0
0.02	0.980	0.980	0.979	0.979	0.979	0.980	0.981
0.05	0.948	0.948	0.948	0.948	0.948	0.947	0.947
0.1	0.896	0.895	0.895	0.896	0.895	0.894	0.893
0.2	0.793	0.792	0.793	0.792	0.792	0.791	0.791
0.3	0.696	0.696	0.696	0.696	0.696	0.697	0.700
0.4	0.606	0.606	0.606	0.607	0.607	0.610	0.618
0.5	0.522	0.521	0.522	0.522	0.523	0.530	0.547
0.6	0.441	0.441	0.441	0.442	0.444	0.459	0.487
0.7	0.362	0.362	0.362	0.363	0.369	0.394	0.437
0.8	0.281	0.281	0.282	0.286	0.297	0.339	0.396
0.9	0.191	0.192	0.195	0.205	0.230	0.293	0.360

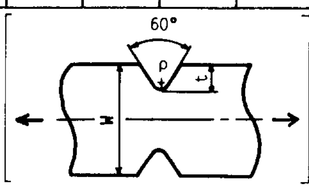

Table 8. Values $K_t/K_t|_{2t/W\to 0}$ in in-plane bending of a strip.

2ρ/W \ 2t/W	0.02	0.03	0.05	0.1	0.2	0.5	1.0
0.02	0.948	0.948	0.947	0.946	0.946	0.948	0.951
0.05	0.881	0.879	0.880	0.879	0.879	0.882	0.886
0.1	0.785	0.784	0.785	0.785	0.787	0.793	0.803
0.2	0.640	0.639	0.640	0.642	0.647	0.662	0.684
0.3	0.530	0.531	0.532	0.536	0.544	0.568	0.599
0.4	0.443	0.444	0.446	0.452	0.463	0.495	0.536
0.5	0.370	0.372	0.375	0.382	0.398	0.437	0.486
0.6	0.308	0.310	0.313	0.323	0.343	0.391	0.445
0.7	0.251	0.253	0.258	0.271	0.295	0.349	0.410
0.8	0.196	0.200	0.207	0.223	0.251	0.314	0.379
0.9	0.138	0.144	0.154	0.175	0.211	0.281	0.351

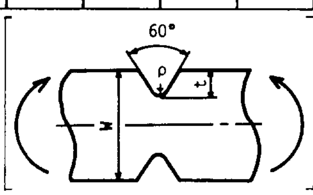

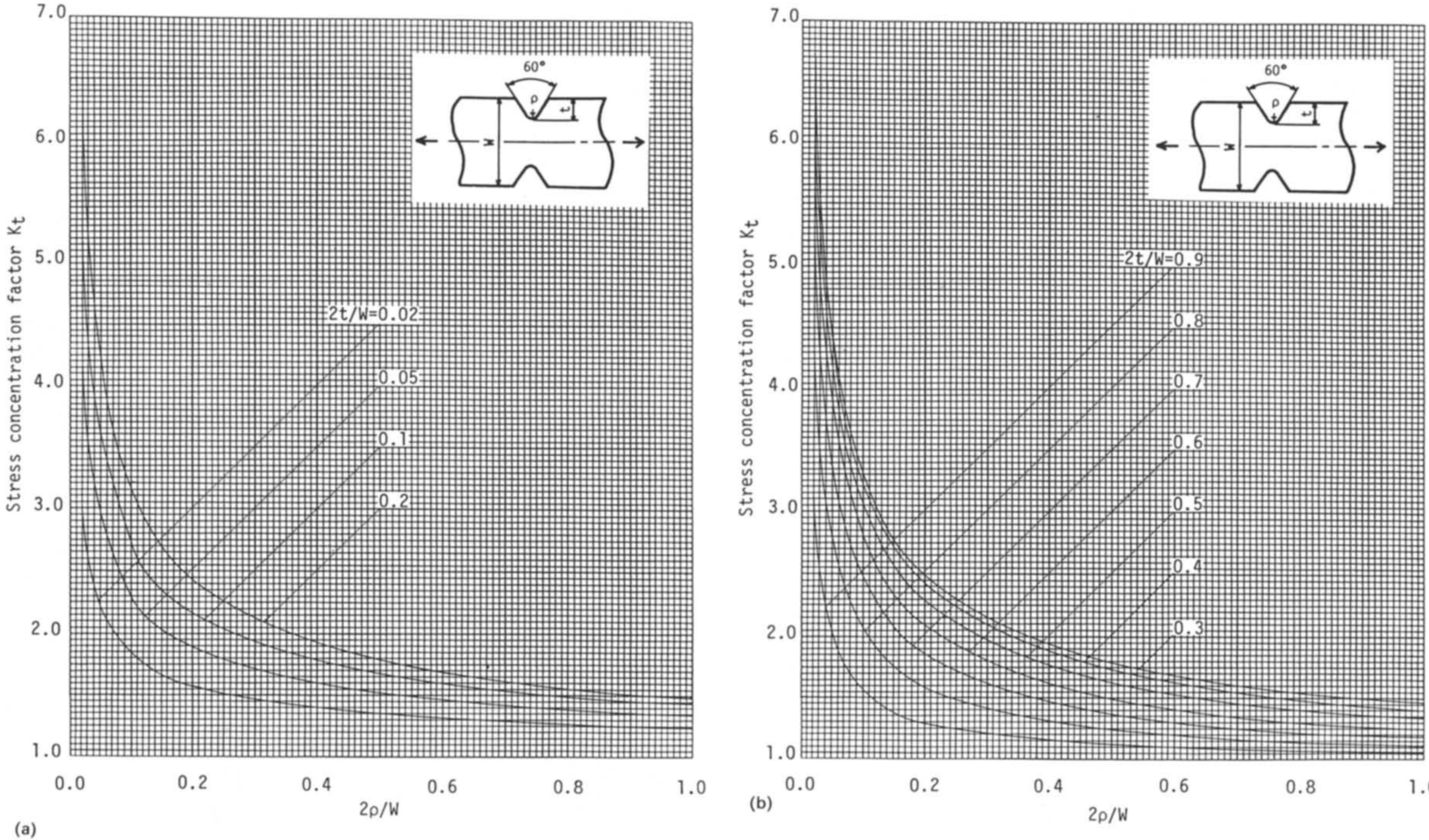

Fig. 7. (a), (b) SCF of 60° V-shaped notches under tension.

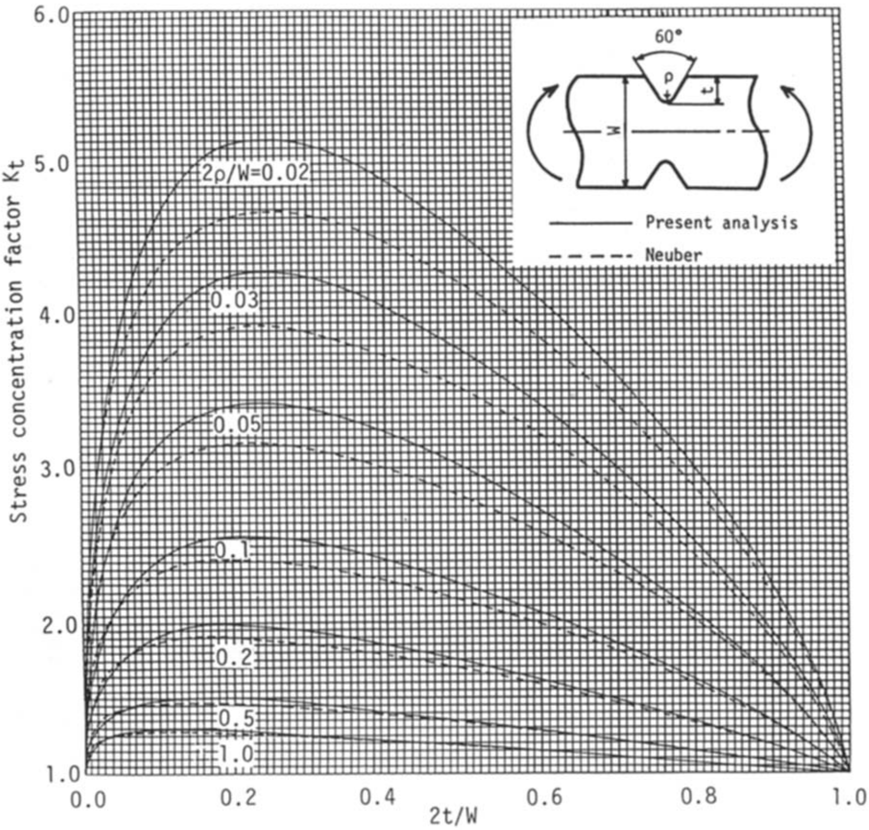

Fig. 8. SCF of 60° V-shaped notches under in-plane bending.

found that the values of K_t/K_{to} are mainly determined by the relative notch depth $2t/W$ alone, especially for shallow notch. Utilizing this fact, we can estimate the SCF of sharp V-notched strip not calculated in this paper ($2\rho/W < 0.02$). The procedure is summarized as follows.

Step (1). Obtain the SCF of the given V-notch in a semi-infinite plate (K_{to}) using the results shown in the Appendix.

Step (2). The value K_t/K_{to} is obtained from the value $2t/W$ by using Tables 7 and 8.

Step (3). The SCF of the given V-notch in a strip is given by the equation: $K_t = K_{to} \cdot (K_t/K_{to})$.

5. CONCLUSION

In this paper, the stress concentration problems of a double V-notched strip under tension and in-plane bending were analyzed by the body force method. The conclusions can be summarized as follows:

(1) In the present analysis, the Green's function of a semi-infinite plate was used as a fundamental solution for strip problems. The method is convenient for systematic calculation of stress concentration factors because the Green's function is given in closed form. The present results for semicircular notch are in close agreement with the other paper's results.

(2) Stress concentration factors K_t of 60° V-shaped notch and of partially-circular notch were systematically calculated under various geometrical conditions. The Neuber formula is found to give an underestimated stress concentration factor of about 11% for tension case and in 9% for bending case. These errors exist for a wide range of notch depth. However, for blunt notches, the Neuber solution of deep hyperbolic notches gives a sufficient accuracy in engineering use.

(3) The values $K_t/K_{to}(K_{to} = K_t|_{2t/W\to 0})$ are found to be mainly determined by the relative notch depth $2t/W$ alone. Taking account of this point, the K_t values of extremely sharp notch in a strip not calculated in this paper can also be estimated from the values of K_{to}.

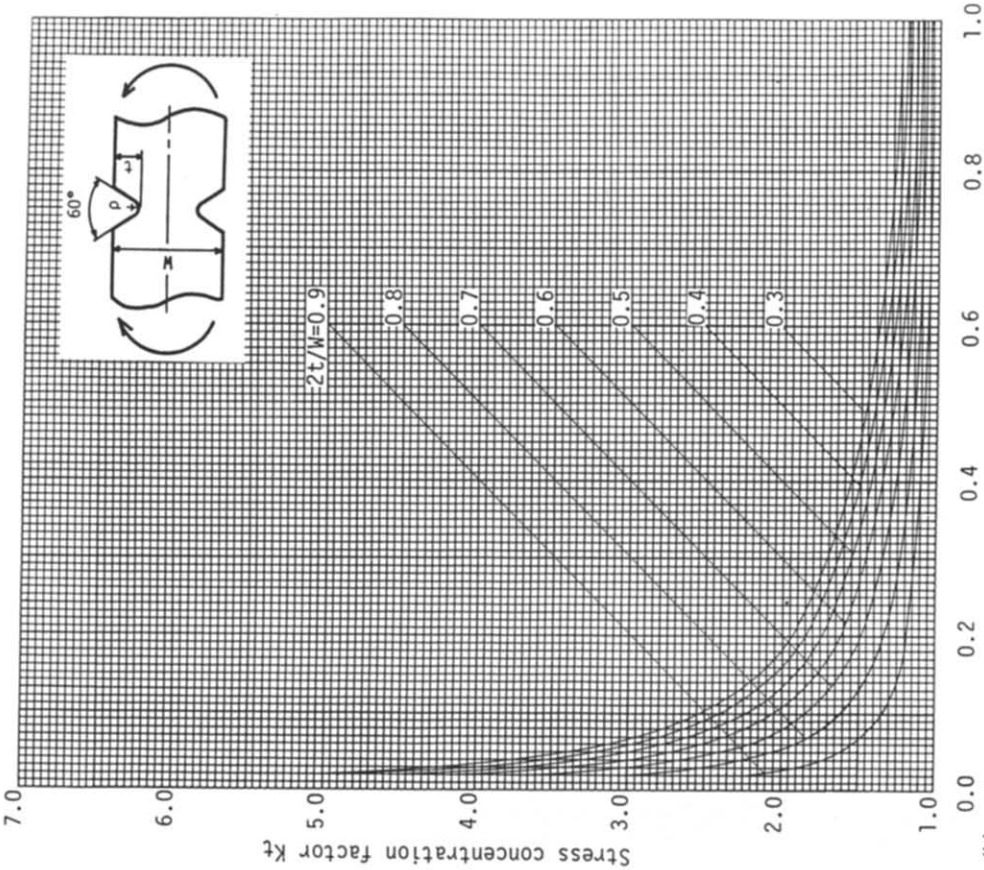

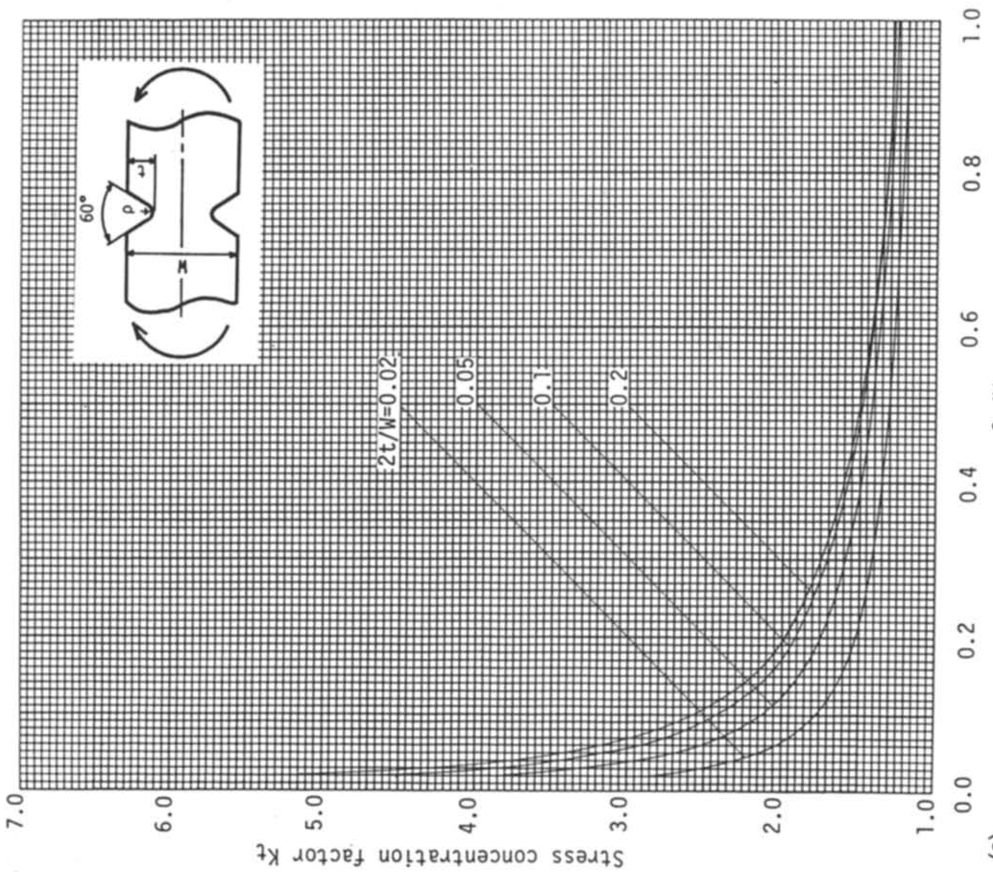

Fig. 9. (a), (b) SCF of 60° V-shaped notches under in-plane bending.

REFERENCES

[1] C. B. Ling, Stresses in a notched strip under tension. *J. Appl. Mech.* **14**(4), 275–280 (1947).
[2] C. B. Ling, On the stresses in a notched strip. *J. Appl. Mech.* **19**, 141–146 (1952).
[3] C. B. Ling, On stress-concentration factor in a notched strip. *J. Appl. Mech.* **35**, 833–835 (1968).
[4] O. Tamate, Stresses in infinite strip with a semi-circular notch under uniform tension and pure bending. *Technol. Rep. Tohoku Univ.* **16**, 34–53 (1952).
[5] M. Isida, On the tension of the strip with semicircular notches. *Trans. Japan Soc. Mech. Engrs (JSME)* **19**, 5–10 (1953).
[6] M. Isida, On the bending of a strip with semicircular notches. *Trans. Japan Soc. Mech. Engrs (JSME)* **19**, 94–99 (1953).
[7] A. Atsumi, Stress functions for an infinite strip with semicircular notches. *Trans. Japan Soc. Mech. Engrs (JSME)* **19**, 94–99 (1953).
[8] M. M. Frocht, Photoelastic studies in stress concentration. *Mech. Engng* **58**, 485–489 (1936).
[9] M. Kikukawa, A note on the stress-concentration factor of a notched strip. *Proc. 3rd Cong. Theor. Appl. Mech.*, pp. 59–64. India (1936).
[10] H. Nisitani, Tension of a strip with symmetric edge cracks or elliptic-arc notches. *Trans. Japan Soc. Mech. Engrs (JSME)* **41**, 2518–2526 (1975).
[11] N. Hasebe and Y. Horiuchi, Stress analysis for a strip with semi-elliptical notches or cracks on both sides by means of rational mapping function. *Ingenier-Archiv* **47**, 169–179 (1978).
[12] H. Neuber, *Kerpspannungslehre*. Springer-Verlag, Berlin (1958).
[13] H. Nisitani, The two-dimensional stress problem solved using an electric digital computer. *J. Japan Soc. Mech. Engrs (JSME)* **70**, 627–632 (1967). [*Bull. Japan Soc. Mech. Engrs (JSME)* **11**, 14–23 (1968).]
[14] H. Nisitani, Solution of notch problems by body force method. *Stress Analysis of Notched Problems* (Edited by G. C. Sih), pp. 1–68. Noordhoff, Leyden (1978).
[15] H. Nisitani and N. Noda, Stress concentration of a cylindrical bar with a V-shaped circumferential groove under torsion, tension or bending. *Engng Fracture Mech.* **20**, 743–766 (1984).
[16] H. Hasegawa, Tension of a strip with semicircular notches (solution by using Green's function of a strip). *Prepr. Japan Soc. Mech. Engrs (JSME)* **840**, 80–82 (1984).
[17] H. Nisitani and N. Noda, Study on the stress concentration problem of a cylindrical bar having a 60° V-shaped circumferential groove under tension. *Trans. Japan Soc. Mech. Engrs (JSME)* **51**, 54–62 (1985).

(*Received* 3 *June* 1985)

APPENDIX

Stress concentration factors of a 60° V-shaped notch in a semi-infinite plate can be also calculated by the body force method. These values are utilized for estimating the SCFs of a sharp notch in a strip from the previous discussion in Section 4.3. In Table A1, the K_t values of a 60° V-shaped notch (K_{tV}) in a semi-infinite plate are shown for a wide range of t/ρ. SCFs of a semi-elliptical notch (K_{tSE}) and of an elliptical hole (K_{tE}) are also shown to be compared with the K_{tV} values.

The ratios of K_{tV}/K_{tE} and of K_{tSE}/K_{tE} are plotted in Fig. A1, where the abscissa represents $\sqrt{(t/\rho)}$. As $\sqrt{(t/\rho)} \to \infty$, we know the ratio K_{tsE}/K_{tE} tends to approach the value for crack case 1.1215. On the other hand, the ratio of K_{tV}/K_{tsE} tends to approach the value K_{tV} / $K_{tSE} \cong 1.04$ as shown in Fig. A2. Using these charts, we can estimate the SCF of a 60° V-shaped notch for all ranges of $\sqrt{(t/\rho)}$.

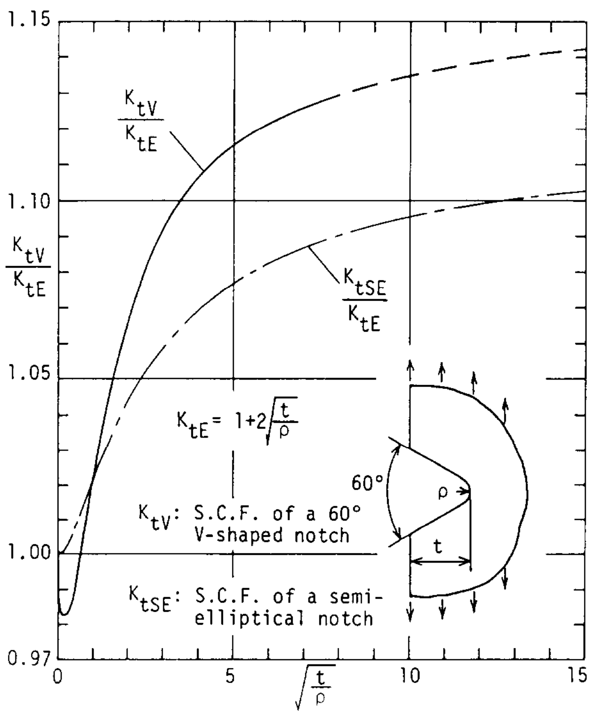

Fig. A1. Values K_{tV}/K_{tE} and K_{tSE}/K_{tE} in tension of a semi-infinite plate.

Table A1. SCFs of a 60° V-shaped notch in a semi-infinite plate.

$\frac{t}{\rho}$	$\sqrt{\frac{t}{\rho}}$	K_{tV}	K_{tSE}	K_{tE}
0.0625	0.25	1.474	1.503	1.5
0.25	0.5	1.983	2.016	2
1	1	3.065	3.065	3
2	1.414	3.995	3.951	3.828
4	2	5.331	5.221	5
8	2.828	7.243	7.036	6.657
16	4	9.958	9.623	9
36	6	14.58	14.07	13
64	8	19.20	18.53	17
100	10	23.8	23.00	21
225	15	35.4	34.19	31
400	20	47	45.39	41

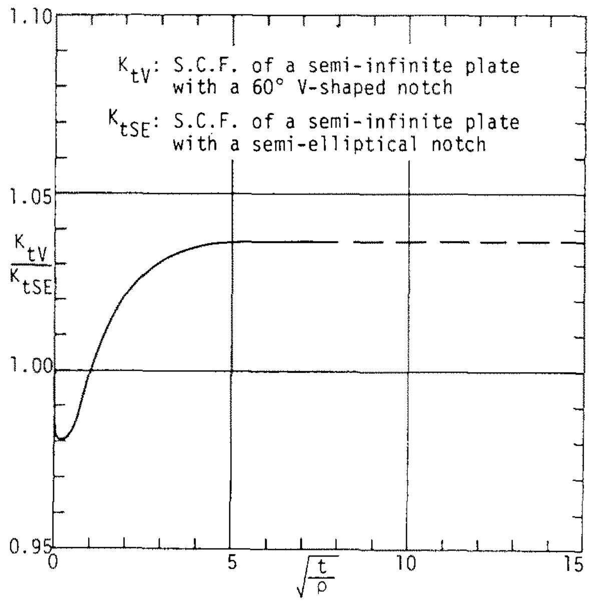

Fig. A2. Values K_{tV}/K_{tSE} in tension of a semi-infinite plate.